Journal of Korean Institute of surface Engineering
Vol. 29, No. 5, Oct., 1996

THIN FILM TECHNOLOGIES RELATED TO THE HIGH T_C SUPERCONDUCTORS

Ri, EuiJae (Eue-Jae Lee)

Korean Academy of Industrial Technologies
GaJwaDong, SeoGu, InCheon 404-254, DaeHanMinGuk

ABSTRACT

Thin film technologies for fabricating SQUIDs involve etching and deposition procedures with the proper substrate materials and $YBa_2Cu_3O_{7-d}$ (YBCO) as the high T_C superconductor. YBCO were prepared on various substrates of MgO, $SrTiO_3$, and $LaAlO_3$ by using off-axis magnetron sputtering methods and annealing in-situ. The parameters of film fabrication processes had been optimized to yield good quality films in terms of the critical temperature T_C and the critical current density J_C.

The optimized processes yielded $T_C>90K$ along with $J_C>10^6A/cm^2$ at 77K and $>2\times10^7A/cm^2$ at 5K. We fabricated step-edge type dc-SQUIDs and directly coupled magnetometers, producing step edges on MgO(100) substrates by etching with Ar-ion beam, depositing YBCO material on them, then patterning them by using ion-milling technique. Circuitizing washer-shape SQUIDs to possess a pair of step-edge junctions of 2-5μ line width with a high angle$>50°$, we examined their I-V characteristics thoroughly and Shapiro steps clearly as we irradiate microwaves of 8-20 GHz frequency.

INTRODUCTION

Commercialization of thin film high temperature superconductors has been started[1] already; Josesphson junctions and SQUIDs as eloquent microelectronic devices have been successfully fabricated by many researchers[2-7] utilizing these materials. Step-edge junction (SEJ) formed around a purposefully prepared grain boundary has advantages over others. It can be made on any arbitrary position of the substrate while bi-crystal junction has restrictions inheritantly. Compared with bi-crystal or other multi-layer juctions, its fabrication processes are rather simple and its strength can be varied easily by a simple design change.

Most important factors in manufacturing this SEJ are, of course, the sharpness and evenness of the step-edge. When a film of YBCO grows in c-axis orientation epitaxially from the substrate surface, various grain boundaries[8-10] form depending on the angle and height of step. With a step angle $> 60°$, a 90° grain boundary is formed only in a case that the step height is larger than the film thickness; if the angle is less than 40 degrees the film grows vetically oriented in c-

axis no matter what the film thickness or step height is and no grain boundary is formed; and with the angle in between the grain boundary becomes complex as observed by using a HRTEM[8-11].

Making a good quality step-edge on a substrate of such metallic oxide as $SrTiO_3$ (STO), $LaAlO_3$ (LAO) or MgO is not easy[12], since a RIE method cannot be used without proper reactive gas for these materials formed yet. Wet chemical etching method normally prouces a low angle step[13] and tends to deteriorate[14] the surface characteristics of YBCO and STO. Thus, dry ethcing method is preferable. One possible way is to use ion milling method, although the etching rates of these materials are as slow as 3 to 4 times less than that of silicon. For this work, an ion milling using argon as the working gas was selected in making SEJ-SQUIDs and magnetometers on the substrates of MgO and STO.

It is noted, though, that STO and LAO are expensive materials and the dielectric constant of STO is too high (e=1900 at 77K) as for an electronic device. The commercialization being kept in mind, MgO would be the best choice if the YBCO film that has been deposited on it showed reasonably good characteristics; an emphasis was placed, thus, on this material throughout this work.

EXPERIMENTAL PROCEDURE

In this work, two ion milling systems employed, those set-ups will not be described in detail here though because it has been done elsewhere[14]. The step was designed to position in the middle of substrate. As the milling mask, photo resists (PR) Az 1512 or 1518 and niobium thin film were employed. In order to prevent the PR mask to erode at corners, instead of hard baking after the development, the PR was exposed to ultra violet for 30 seconds as a soft baking process. This may increase the molecular weight to a reasonable value, so decrease the erosion possiblility. Nb has an advantage in making a sharp edge, owing to the thinness and low milling rate. Fabrication process for Nb mask is as follows : The patterned Az 1518 PR was soaked in chlorobenzene to render undercuts. Nb was deposited about 400 nm in an rf sputtering machine. Then, the PR was lifted off to leave the completed mask.

Thermal grease was used to attach the substrate onto the copper block being cooled with flowing water to prevent the heat accumulation on the substrate in the milling chamber. The incident ion beam was directed toward the specimen surface with an angle, which was varied from 0 to 50° in an effort to find the optimized condition. For the milling, 400-500 volt energy ion beam was utilized along with 60 mA beam current for both substrates of MgO(100) and STO.

After milling, the substrates were cleaned in an ultrasonic bath with acetone and ethanol, each for 10 minutes to remove PR completely. Then, the steps were closely examined with an SEM and/or AFM.

For the single target magnetron sputtering, various targets[15] with chemical compositions of $YBa_2Cu_xO_y$ where $3 \leq x \leq 6$ were employed to produce YBCO sample films. During the in-situ fabrication process, the substrate temperatures have been kept within a range between 600 and 850℃. The plane magnetron set-up has been described in ref. 15, along with the deposition conditions and proce-

dures, in detail.

Another unit equiped with a hollow cathode type target, so called inverted cylindrical magnetron sputtering (ICMS)[16] has also been employed in an effort to improve the deposition rate. For this equipment, a dc power supply with a capacity of 1 KW was utilized. The procedures for film preparation have been well described in ref. 17.

The base pressure of vacuum chamber was kept as 10^{-6} Torr using a diffusion pump, before Ar and O_2 gases were introduced up to 100-350m Torr for the deposition process and the diffusion pump was turned off while the rotary pump was yet left on. The partial pressure of Ar was allowed as 80 to 250m Torr and the ratio between the two was adjusted as 2-4. The substrate temperatures were maintained within a range of 700-770 ℃. With a bias voltage varying between 145 and 160V (the equipment power 45-75W) and the distance between the substrate and the bottom of cylindrical target within a range of 20 to 30㎜, the deposition process was continued for 24-180minutes to produce a film thickness of 120-600 nm.

The film growth was calculated as 2-5 nm /min in average. After deposition oxygen was introduced into the vacuum chamber for its partial pressure up to 600 Torr until the specimens were cooled quickly to 450℃ in 20minutes and kept there for one hour, then cooled down to the room temperature. Each sample was examined to clarify its characteristics in terms of Tc and Jc afterwards. For the surface conditions. various analysis equiments as AFM, SEM, and Alpha Step were employed to investigate. XRD was also utilized to examine the crystallinity of film samples.

Thin films of YBCO being deposited with a typical thickness around 120-180nm, they are to be dry etched again by using Ar-ion milling technique to patternize for the junction bridges, SQUIDs, and magnetometer samples. Finally, the samples were subjected to examinations for I-V characterization along with microwave irradiation.

RESULTS AND DISCUSSION

Fabricating the Step-Edge

As ion milled with a beam energy 400 or 500eV, incident vertically to the sample surface, the milling rate data are obtained for various materials and collectively shown in Table 1. The flux density was about 2㎃/㎠. Milling rates were further studied with varying the incident angles. Normally the rate increases monotonically[15] as the beam angle increases, as seen Fig. 1.

In order to examine the step slope of MgO fromed by ion milling, an SEM was employed to observe the steepest angle $> 50°$, which was produced with the beam angle 10°. Fig 1 also shows a typical example, the plot of step angles obtained with varied beam angles from 0 to 45° while keeeping the beam energy constant as 400 eV. From here, it is obvious to keep the incident angle as 10° for the steep angle of step-edge. For STO substrate, the incident angle 15° yielded a reproducible sharp step with its angle $> 65°$.

Ion milling of STO to make a step resulted

Table 1. Ar-ion Milling Rates in nm/min Obtained

	Materials				
Beam energy(eV)	STO	MgO	YBCO	PR	Nb
400	13	15	38	23	20
500	10	12	44	27	23

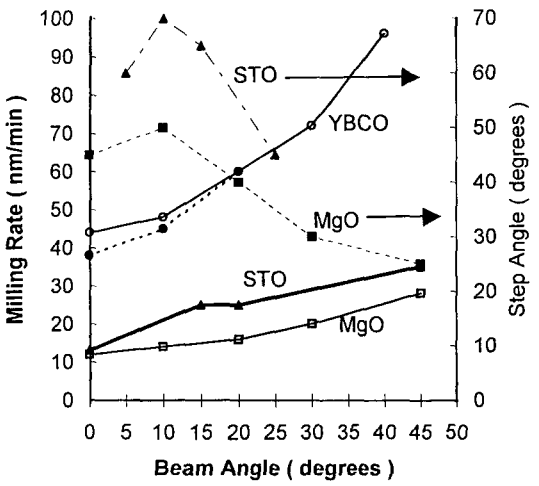

Fig. 1. Milling rates and step angles plotted for various materials as a function of the incident angle of Ar-ion beam. Open symbols represent data obtained with beam energy 500eV, while closed ones obtained with 400eV. Real lines and a dotted line depict the milling rates and broken lines stand for the step angles observed.

sensitively in the step angle produced, depending on the changes of beam angle and ion energy. Particularly for PR as the milling mask small difference during photolithography process yielded a significant variation in the step angle. This is considered owing primarily to the masking material[18]. While numerous steps with different heights in a range of 150 to 800 nm were produced. the best result was obtained with a step height 200 nm and its typical step angle about 60 to 70°.

The steps were examined also with AFM non-destructively for the morphology of sample surface. Fig. 2 depicts the AFM images of juction area pattened on a STO substrate, showing the step angle being 65°. The film of YBCO is seen to cover fairly uniform on the step region.

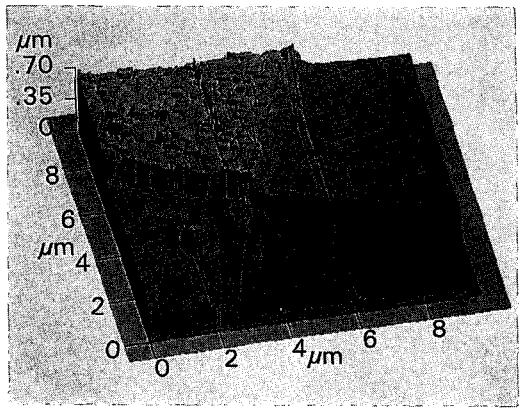

Fig. 2. AFM image of the step juction area showing the step angle of 65 degrees.

For the sharp step (Fig. 2), a-axis oriented platelike paticles are observed at the step-edge region. It is concluded that the substrates prepared with PR or Nb can produce steep and straight edge lines as long as the milling parameterers are met reasonably.

Sputter Deposition for YBCO Thin Films

While various composition targets were tried to obtain the stoichiometric thin film of YBCO on MgO with the relatively high value of T_C, it was found for the plane magnetron process that the composition ratios of Ba/Y and Cu/Y to be 1.8 and 3.7, respectively, produced best results. Pre-experimental runs with a 123-target confirmed that the proper value of Ptotal must remain within a range from 100 to 300 m Torr as combined with the distance from substrate to target, D_{s-t} to be 40(horizontal)+42(vertical)㎜.

To find the optimized condition, "Follow the Local Maxima" strategy was utilized for the best resuting T_C; firstly a set of experimental runs were carried on with a major parameter varied within a reasonable range

Table 2. Tsub Varied for the Sputtering Process Optimization Scheme (Ptotal = 200mTorr, Ar/O_2 Ratio=3, Power= 110W, D_{s-t}=40+42mm)

T_{sub}(℃)	740	750	755	760	765	770	780
Bias(V)	44.5	21.6	18.0	19.1	18.2	17.6	20.0
T_C(K)	62.8	83.0	83.1	84.2	84.3	85.0	72.1

while others fixed to find the local best in T_C, then the second parameter was chosen to vary while fixing the others, etc. In this optimization scheme, first several substrate temperatures for MgO were selected from the range of 740-780℃. Table 2 shows the values of T_{sub} and the corresponding proper bias voltages that ranged between -17.6 and -44.5volts during each deposition run. For this set of experiments, other parameters than T_{sub} were fixed as : P_{total}=200mTorr, Ar/O_2 Ratio=3, and Power=110W. The thickness of the films was kept constant at 200nm throughout this work. The averages of T_C values measured after each run are shown also in Table 2. It is obvious here that the first local maximum T_C=85K has occured at T_{sub} = 770℃.

Next set of experiments was performed with the values of Ar/O_2 gas ratio varied within a range of 1 to 15, fixing T_{sub} as 770℃ but the rest of parameters same as the first set. During this period of time the bias ranged from -10.0 to -20.1 volts, of which each case is arranged in Table 3 along with its resulting T_C value. Table 3 clearly depicts the second local maximum T_C=86.3K to have taken a place with a ratio Ar/O_2=9.

Table 3. Ar/O_2 Gas Ratios Varied for the Sputtering Process Optimization (Tsub=770℃, Ptotal=200mTorr, Power=110W, D_{s-t}= 40+42mm)

Ar/O_2	1	3	5.5	9	12	15
Bias(V)	20.1	20.0	12.6	11.5	10.2	10.0
T_C(K)	85.0	85.4	85.5	86.3	84.9	17.0

Final set of experiments for the optimization scheme was run by varying the chamber pressure P_{total} within a range of 100-300 mTorr and by keeping Ar/O_2=9. The applied bias was varied from -23 to -12volts as P_{total} was increased. The data of T_C obtained from these samples are plotted against the corresponding P_{total} values, in Fig. 3.

Fig. 3 clearly shows that the final maximum Tc of 90K has been reached with P_{total} being kept at 150mTorr. It is important to point out that -20V dc bias was possible for the run to yield good film surface condition. From the samples examined under an SEM, we observed excellent surface morphology that would affirm the high quality of film

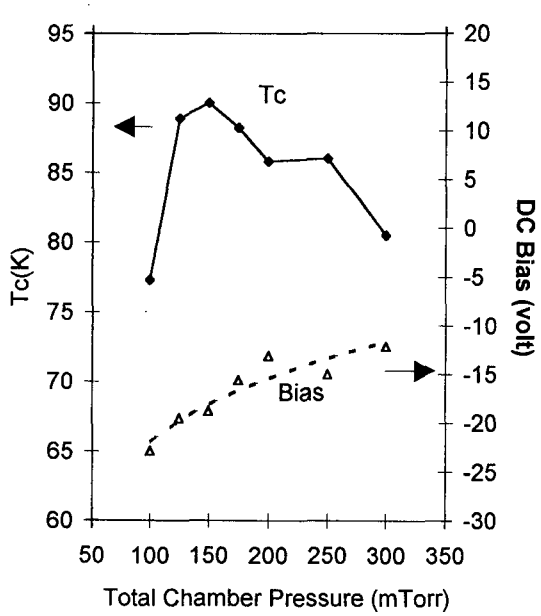

Fig. 3. Plot of T_C and DC bias vs. total chamber pressure for the samples processed at T_{sub} =770℃ and Ar/O_2 ratio=9.

product. In addition, YBCO films[15] synthesized on MgO with ICMS at the substrate temperature 725℃ recorded the value of Tc a little higher than 90K. Some other sample films that were produced on LAO and STO showed T_C in the range of 85-90K. These results are well compared with the T_C of YBCO crystals[19] and considered good enough to further proceed to next procedures.

A four-probe multimeter unit, directly applied to the film samples on MgO substrate in order to measure the values of current flowing across them, rendered the values of J_C being larger than 2×10^7A/㎠ as examined at T=5K without magnetic influence. When these samples were subjected to a temperature T=77K with H=0 Tesla, they showed the values of Jc larger than 1×10^6 A/㎠. Crystallinity of the film specimens was also

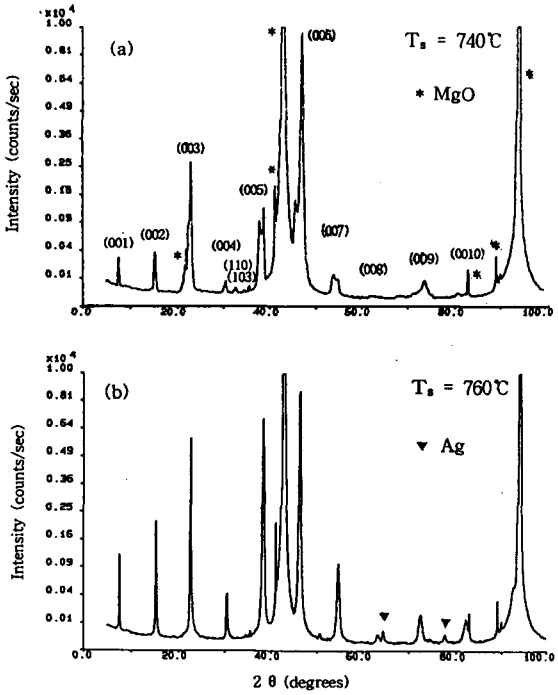

Fig. 4. X-ray diffraction patterns of the films deposited at (a) 740℃ and (b) 760℃ under the pressure of 200 mTorr.

investigated with an X-ray. As shown in Fig. 4, a typical film grown at 740℃ revealed that the 123-YBCO phase was formed incompletely. Meanwhile, others grown at temperatures between 760 and 780℃ demonstrated their completeness through such crystal orientation as{00l} peaks in the XRD spectra which prove that the 123 grains were grown along the c-axis epitaxially (see Fig. 4). These results, therefore, ensure us that the thin YBCO films grown on MgO substrate could be comfortably used in manufacturing electronic devices because of MgO possessing strong chemical stability and excellent dieletric property, as compared with other substrate materials like STO and LAO[15].

The YBCO thin films were prepared c-axis oriented except at the step-edges by using the off-axis magnetron sputtering. The typical film thicknesses of 120-180 nm were obtained. The T_C values ranged from 88-90K, while critical current densities were measured in exess of 3×10^6A/㎠ at 77K routinely. Resistivities at 100K were around 80 μohm-㎝, while the transition widths were outstandingly less than 1K.

Dry Etching for Patterning YBCO

It was carried out with a milling mask produced by using a standard photolithography after applying PR to the YBCO film. As shown in Fig. 1, the milling rate as beam angle=0 and E(beam)=500eV was as fast as 0.8nm/sec. As the angle was varied to 45°, the milling rate increased linearly as the angle did. At this angle, the rate recorded 1.6nm/sec, which is twice the value for the case of beam angle=0.

The thin YBCO films deposited on STO and

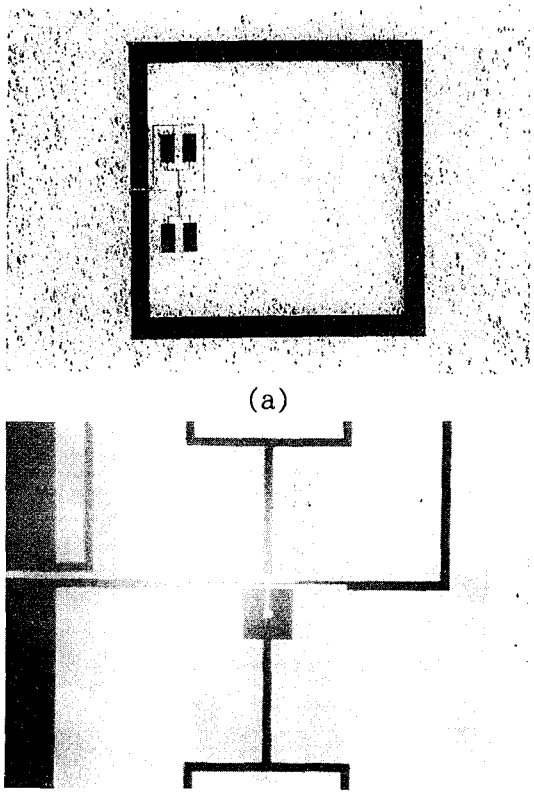

Fig. 5. Diretly coupled magnetometer; a) an overall view and b) a close-up view for the SQUID.

MgO substrates were patterned to fabricate Josephson junctions and SQUIDs[20]. The films were milled to form a line width down to 2 microns. Charaterization activities revealed that there was no degradation in terms of the transition temperature or the critical current density of specimens. These results were reproducible.

Fig. 5 shows the photos for a directly coupled magnetometer and a washer-type dc-SQUID that are patterned with ion milling method. In Fig. 5b, the step-edge is clearly seen in the middle of upper half. The microbridges of YBCO cross the step-edge. The process conditions with E(beam)=500eV, beam angle=10° and milling rate=1nm/sec prooved not to damage the step-edge consequently. It was also confirmed that T_c and J_c did not degade, so was the reproducibility of trustful devices.

Charaterization of SQUID and Magnetometer

Microbridges with a line width of 2-5micron were formed near the 240 nm high step-edge in an effort to fabricate a dc-SQUID and a directly coupled magnetometer. Flowing an electric current through these devices, I-V and v-Φ characteristics were examined. The dimension of square washer for the SQUID is $120\times120\mu^2$ while the square hole and slit sizes are $40\times40\mu^2$ and $4\times120\mu^2$, respectively. The specimens were fixed in Cryostat and cooled with liquid helium, to observe their I-V curves. I_c was measured as 30μA at 40K and as temperature dropped the values of Ic increased to be 100 μA at 10K. The Ic values of the SEJ-SQUID and the magnetometer were measured in μA and plotted against the corresponding operation temperatures. A gradual decrease in Ic is obvious after a quick drop in I_c from 20K to 30K, presumably down to zero at the transition temperature around 90K. Interpolation renders the critical current 4.0 μA at the liquid nitrogen temperature 77K. Flux to voltage characteristics of the dc SQUIDs were thorouly examined to find the critical bias current varying the bias current values at a preferable 77K. The critical bias current was obtained as 38 μA.

To confirm the SQUID behaving propely as Josephson junctions by Shapiro steps, this device was subjected to a microwave of 20 GHz

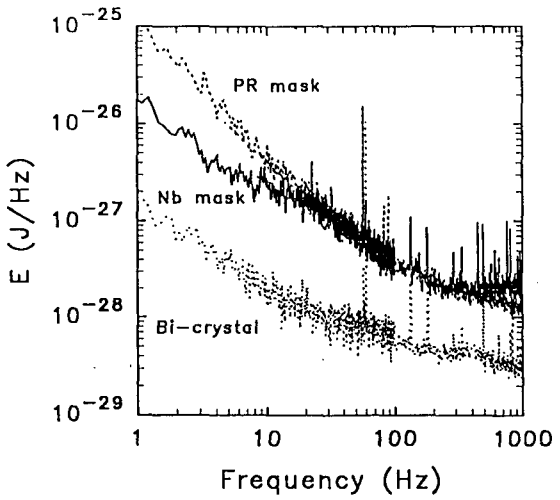

Fig. 6. Flux noise characteristics of a directly coupled magnetometer possessing a SEJ type dc-SQUID

frequency. The microwave power was varied upto 13.5 dB in order to study the effect on the SEJ-SQUID and the frequency was also varied. It was clearly confirmed that the SEJ-SQUIDs depict[14] Shapiro step characteristics as a Josephson juction behavior under the influence of microwave. Then, SQUID magnetometers were subjected to measure the flux noise characteristics. The one fabricated by using a PR mask revealed 2.2×10^{-7} Φ_0^2/Hz at 10Hz frequency level through 7.0×10^{-9} Φ_0^2/Hz at 1KHz frequency level as shown in Fig. 6. This result is comparable with bi-crystal grain boundary SQUID[20], but one order of magnitude higher noise.

CONCLUSIONS

1) Step edges on MgO(100) and STO substrates were neatly produced by etching with Ar-ion beam of 400 V. The critical parameter was the beam incident angle; 10 degrees for MgO substrate but 15 degrees for STO substrate. The best step height was 200 nm and its typical step angle was obtained as 65 degrees.

2) Superconducting films of YBCO were syn-thesized on various substrates of MgO, $SrTiO_3$, and $LaAlO_3$ by using the methods of off-axis magnetron sputtering and annealing in-situ. Deposition results showed a good feasibility with the MgO substrate. The optimized ICMS processes (Base Vac$\sim10^{-6}$ Torr, Partial Pressure of O_2=50 mTorr, P_{Ar}=150 mTorr, T_{sub}=750K, Bias Voltage=145-160V, D_{s-t}=25 ㎜, one hour annealing with Partial Pressure of O_2=600 Torr after furnace cooling to 450 degreeC) yielded T_C>90K along with J_C> 106A/㎠ at 77K and>2×10^7A/㎠ at 5K.

The quality of thin films was good enough to build micro-electronic devices operating at the boiling temperatue of liquid nitrogen.

3) Patterning the YBCO films were carried out successfuly, without degradation, by using ion-milling technique. For the samples with a line width as small as 2microns, milling rate 60nm/min was kept with E_{beam}=500eV and Beam Angle=10 degrees.

4) Circuitizing washer-shape SQUIDs to possess a pair of step-edge junctions of 2-5μ line width with a high angle>50°, we examined their I-V and v-Φ characteristics thoroughly and Shapiro steps clearly as we irradiate microwaves of 8-20GHz frequency.

5) The SQUID magnetometer fabricated by using a PR mask showed the flux noise characteristics as 2.2×10^{-7} Φ_0^2/Hz at 10Hz frequency level through 7.0×10^{-9} Φ_0^2/Hz at 1KHz frequency level.

ACKNOWLEDGEMENTS

The author acknowledges Dr. S. Moon, Messrs. J. Baig and Y. Song, for their special contributions during this work. Much gratitude is extended to Messrs. E. Lee and I. Song at Samsung Adv. Inst. of Tech. for some portions of the tedious laboratory work; also to Prof. Z. Khim at SNU and Drs. J. Lee, T. Park and at SAIT for very helpful discussions.

REFERENCES

1. Superconductor Industry, 9(3), 6 (1996)
2. R. H. Koch, C. P. Umbach, G. J. Clark, P. Chaudhari and R. B. Laibowitz, Appl. Phys. Lett. 51, 200 (1987)
3. P. Chaudhari, et al., Phys. Rev. Lett. 60, 1653 (1988)
4. K. P. Daly, W. D. Dozier, J. F. Burch, S. B. Coons, R. Hu, C. E. Platt, and R. W. Simon, Appl. Phys. Lett. 58, 543 (1991)
5. D. K. Chin and T. van Duzer, Appl. Phys. Lett. 58, 753 (1991)
6. K. Char, M. S. Colclough, S. M. Garrison, N. Newman and G. Zaharchuk, Appl. Phys. Lett. 59, 733 (1991)
7. L. Lee, K. Char, M. Colclough and G. Zaharchuk, Appl. Phys. Lett. 59, 3051 (1991)
8. K. P. Daly, W. D. Dozier, et al., Appl. Phys. Lett. 58,543 (1991)
9. J. Luine, J. Bulman, et al., Appl. Phys. Lett. 61, 1128 (1992)
10. G. Friedl, B. Raos, et al., Appl. Phys. Lett. 59, 2751 (1991)
11. C. L. Jia, B. Kabius, et al., Physica C175, 545 (1991)
12. J. Z. Sun, W. J. Gallagher, et al., Appl. Phys. Lett. 63, 1561 (1993)
13. T. Mitsuzuka, K, Yamaguchi, et al., Physica C218, 229 (1993)
14. E. Lee, J.K.I.M.M. 33(6), 800 (1995)
15. E. Lee, Z. Khim, S. Moon, J. Kim, H. Lee, W. Kang, J. Hong, E. H. Lee, I. Song and C. Moon, "Development of High Quality Thin Film and Manufacturing a SQUID Magnetometer," MITE, (1993)
16. X. X. Xi, G. Linker, O. Meyer, E. Nold, B. Obst, F. Ratzel, R. Smithey, B. Strehlau, F. Weschenfelder, and J. Geerk, Z. Phys. 1374, 13 (1989)
17. E. Lee, Industrial Technologies, 5 (5), 9 (1994)
18. R. E. Lee, VLSI Electronics, Vol. 8 (Eds. Einspurch and Brown), 341, (Academic Press 1984)
19. M. Wu. and C. Chu, et al., Phys. D. W. Lett., 58, 405 (1987)
20. S. Moon, E. Lee, et al., J.K.P.S., 27(5), 562 (1994)